ISSN: 2414-1895 DOI: 10.6919/ICJE.202110_7(10).0080

Numerical Simulation Analysis of Tunnel Surrounding Rock Stability and Control

Nian Liu, Dongyang Xu

School of Resources and Environment, Henan Polytechnic University, Jiaozuo, Henan, China.

Abstract

This article takes a subway tunnel as the research area. Use discrete element numerical simulation software to simulate the stability change of surrounding rock caused by tunnel excavation. The analysis and research on the surrounding rock deformation caused by the method of excavation in the left and right line sequentially, the actual monitoring and simulation are compared and analyzed.

Keywords

Surrounding Rock; Stability; Numerical Simulation.

1. Introduction

Rail transit built underground in cities can make full use of urban underground space; because it has the advantages of fast operation, large passenger capacity, economy and environmental protection, and small impact on existing infrastructure, it can effectively alleviate ground traffic congestion , One of the most effective ways to solve the rapid increase in urban residents and the contradiction between transportation supply and demand [1]. Since the end of the 20th century, the country has further increased scientific research in the field of underground engineering technology. Tunnel traffic and underground engineering have been developed at a high speed. Vigorously expanding underground space will have a great impact on the country's political economy, social security, and environmental protection. The construction and development of all aspects will have extraordinary influence and significance [2-3].

With the increase of shield tunneling distance, the following rules are summarized: surrounding rock stress field, the maximum value of vertical effective stress appears at the position of the arch foot on both sides of the tunnel, and the maximum value of horizontal effective stress appears at the position of the arch waist on both sides of the tunnel . In the surrounding rock displacement field, when the shield cutterhead is about 16m away from the monitoring surface, the stratum in front of it begins to be disturbed and deformed. When the cutterhead passes through the monitoring surface about 48m, the stratum deformation in the disturbed zone tends to stabilize and the stratum reaches the maximum settlement.

2. Project Overview

The landform of the site is a plain formed by alluvial deposits in the Pearl River Delta, and it is also a coastal sedimentary area. The terrain is relatively flat and the height difference is relatively small. The ground elevation along the line is generally -5.4~7.5m, and the maximum elevation difference is 12.9m. The strata from new to old include: Cenozoic Quaternary (Q), Mesozoic Triassic (T). From the perspective of regional geology, from the new to the old, it is as follows:

2.1 Quaternary strata

The Quaternary includes the Holocene (Q4) and the Upper Pleistocene (Q3), and the Middle Pleistocene and the Lower Pleistocene are missing. The Quaternary consists of artificial fill layer

ISSN: 2414-1895 DOI: 10.6919/ICJE.202110_7(10).0080

(Q4ml), sea-land alternate facies silt, sand (Q4mc), etc., alluvial sand, soil layer (Q3+4al+pl) and residual soil layer (Qel), covering the foundation Above the rock.

2.2 Triassic (granite) rock mass

Late Triassic granites (T3ηγ) are mainly medium-grained granites invaded by the late Valissian period. They are light flesh red, light gray red, light gray, etc., with medium-grained structure and massive structure. The mineral composition is feldspar, quartz, and a small amount Biotite and so on.

3. Calculation principle and model establishment

3.1 Principles of Numerical Calculation of Particle Flow

The particle flow discrete element method in the particle flow discrete element software PFC can not be limited to the amount of deformation, can more conveniently deal with the problems of discontinuous medium mechanics, can effectively simulate the separation and deformation of materials, and intuitively reflect the process and results of its deformation [4-6]. In the particle flow discrete element PFC program, discrete particles are used to simulate the movement and interaction of the actual medium, and walls are used for boundary constraints. The principle of the PFC program is based on the discrete element method, and the model is composed of different particles. In PFC2D (two-dimensional), these particles mainly appear as circles; in PFC3D (three-dimensional), these particles mainly appear as solid spheres. The force on the particle is only the contact part between the particle and the particle or the particle and the wall. When the force is greater than the contact strength between the particles, the particles will separate and the model will be deformed. The movement of particles follows Newton's second law. Under the action of external forces, the system can maintain a static balance, or it may be destroyed, and particle flow may occur [7-9].

3.2 Selection of parameters

In order to enable the numerical simulation to be carried out reasonably, combined with indoor and on-site rock and soil experiments, the physical and mechanical parameters of the rock and soil layer are obtained as shown in the following table: The rock and soil physical and mechanical parameters corresponding to the model are shown in the following table,

Table 1. Physical and mechanical parameters of model rock and soil

Strata Lithology	Layer thickness (m)	Densityg /cm^3	Cohesion kPa	Internal friction angle°	Void ratio	Elastic Modulus MPa	Poisson's ratio
Silty soil	7.9	1.66	6.4	6.3	1.346	3.6	0.34
Silty clay	1.7	1.92	14.8	12.0	0.83	10.8	0.31
Coarse sand	20.3	2.0	_	32.0	_	9.5	0.25
Sandy clay	5.9	1.95	23.0	18.0	0.547	7.6	0.29
Strongly weathered granite	7.4	2.30	40	25.0	0.727	20.3	0.18

3.3 Model establishment

Using the PFC command stream, the soil layers with similar physical and mechanical properties are simplified, and a numerical simulation model is established by selecting the shield machine from just entering the lower Hengli waterway to passing through the middle section of the lower Hengli waterway. The entire section of the tunnel is driven by shield tunneling. In the long-term consolidation and settlement process, since each boundary of the model is relatively far from the tunnel, the pore water pressure is basically the same as the static water pressure, so except that the pore water pressure inside the segment is set to zero , And the rest of the boundaries are set as permeable boundaries [10]. When simulating shield tunneling, the excavation footage with the same width as the segment ring is used, a ring of soil is excavated to assemble the segment of the previous ring, and supporting parameters are applied to the segment. When the seepage mode is closed, calculate the deformation of the soil layer in the mechanical mode when it is undrained, and use iterative calculation to make the model reach a mechanical equilibrium state. Then turn on the seepage

ISSN: 2414-1895 DOI: 10.6919/ICJE.202110_7(10).0080

mode, and use the fluid-solid coupling method to calculate the drainage deformation of the model in the seepage mode and the mechanics mode. After calculating the convergence balance, excavation of the next ring is carried out, and the excavation is repeated in this way until the end of the excavation. The initial model is shown below:

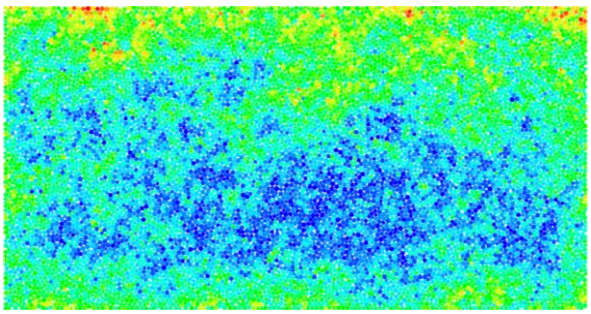

Figure 1. Initial model of the model

4. Numerical simulation analysis of surrounding rock stability and control

4.1 Analysis of surrounding rock stress field

When the tunnel is not excavated, the initial stress field is generated under the interaction of its own gravity and tectonic stress. The initial stress has a very important influence on the excavation of the tunnel. The initial site stress is also one of the important factors that cause deformation and damage when the environmental conditions of the rock mass change. Under the condition that the shield machine traverses 13m deep river water and has stable seepage, the effective stress in the vertical direction gradually increases horizontally and symmetrically from top to bottom according to the change of the soil layer. The effective stress in the horizontal direction is basically the same as the effective stress in the vertical direction, and is also distributed symmetrically in the horizontal direction. Due to the disturbance of the rock and soil mass caused by the excavation of the shield machine, the initial state of the surrounding rock of the tunnel has been destroyed, and the magnitude of the effective vertical stress has changed significantly, especially the change of the stress field near the tunnel excavation surface. Significantly. With the excavation of the shield, the vertical stress field gradually forms a funnel-shaped distribution above the tunnel, and the vertical stress at the top of the tunnel is significantly higher than other parts. With the increase of the driving length, the vertical stress of each monitoring surface at the top of the tunnel gradually increased, and the radius of the funnel also increased, but the impact on the stress at the top of the model was not too obvious.

After the excavation of the right line, it also had a greater impact on the tunnel excavated on the left line, resulting in a greater increase in the stress on the top of the left line tunnel. With the excavation of the right line, the stress field funnel on the top of the tunnel changes from one on the left line to two, and with the increase of the length of excavation, the stress field funnels at the top of the left and right line tunnels are distributed symmetrically with the central axis as the axis of symmetry. Similar to the excavation of the left line alone, the longer the excavation length is, the radius of the stress field funnel also tends to increase. The maximum value of the vertical effective stress is mainly distributed in the arch waist of the tunnel.

4.2 Analysis of surrounding rock displacement field

The influence on the surrounding rock displacement field is mainly reflected in the vertical displacement and horizontal displacement, and with the change of the tunneling length, the influence on the vertical displacement and the horizontal displacement is different. After the excavation of the shield tunnel, the surrounding rock at the top of the vault undergoes tensile failure to produce settlement displacement, the bottom of the arch produces uplift and rebound deformation, and the left and right arch waist produce symmetrical horizontal displacements and are close to the center of the

ISSN: 2414-1895 DOI: 10.6919/ICJE.202110_7(10).0080

tunnel. The following three figures are the vertical and horizontal displacements of the tunnel at the initial stage of excavation, as well as the model diagrams of the total displacement.

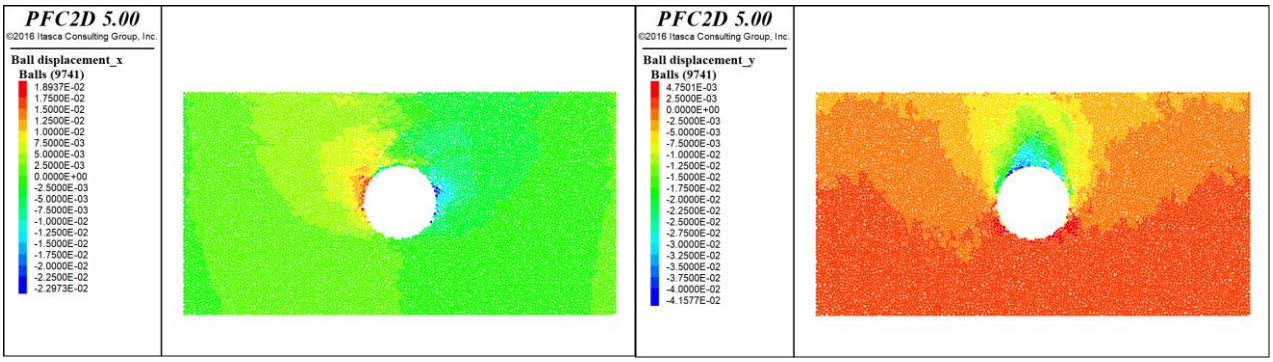

a. Horizontal displacement b. Vertical displacement

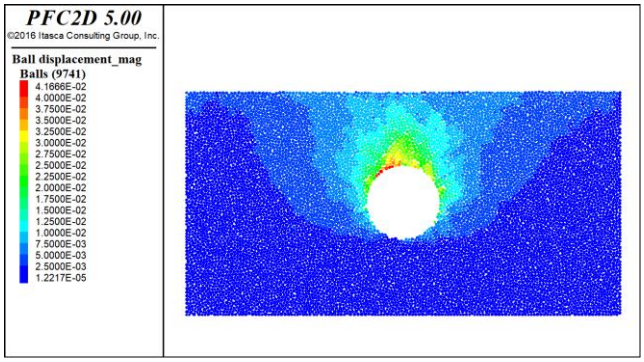

c. Total displacement

Figure 2. Model displacement diagram

From the numerical simulation of the vertical displacement cloud diagram of the above figure, it can be found that when the shield tunnel is just started, the settlement of the dome increases continuously with the increase of the number of excavation loops, and the degree of influence gradually decreases from the top to the bottom of the dome; in the left tunnel The impact of the excavation on the top and bottom of the arch spreads outward in a "bulb" shape, and is basically symmetrical up and down to the river bottom and strongly weathered granite respectively. The maximum dome settlement of the monitoring surface is about 4.15mm. Due to the vertical deformation of the surrounding rock of the tunnel, ground settlement will also appear on the ground surface, and the settlement is symmetrical with the tunnel axis "U"-shaped settlement trough, and with the increase of the tunnel length, the shape of the settlement trough gradually changes from the "U" shape Transforming to a "V" shape, the rate of change of surface subsidence has also increased. The horizontal displacement is significantly reduced compared with the vertical displacement, the maximum horizontal displacement is 2.29mm, and the maximum total displacement is 4.16mm. It can be seen that the vertical displacement mainly affects the total displacement, that is, the displacement of the dome settlement is the main influencing factor.

4.3 Analysis of the laws of surface subsidence and stratum deformation

After the surrounding rock of the tunnel is disturbed and deformed, the transmission of the deformation effect will cause the corresponding deformation of the overlying stratum, which is mainly divided into two directions: vertical and horizontal. By setting monitoring points on the three monitoring surfaces of the shield tunneling stage, the impact of left-line excavation and right-line excavation on formation deformation was compared and analyzed. The monitoring points on the monitoring surface are arranged according to the density of shield tunneling at 1, 15, 25,...265, 278 time steps, and import the recorded data into Excel to draw a graph for comparison and analysis

ISSN: 2414-1895 DOI: 10.6919/ICJE.202110_7(10).0080

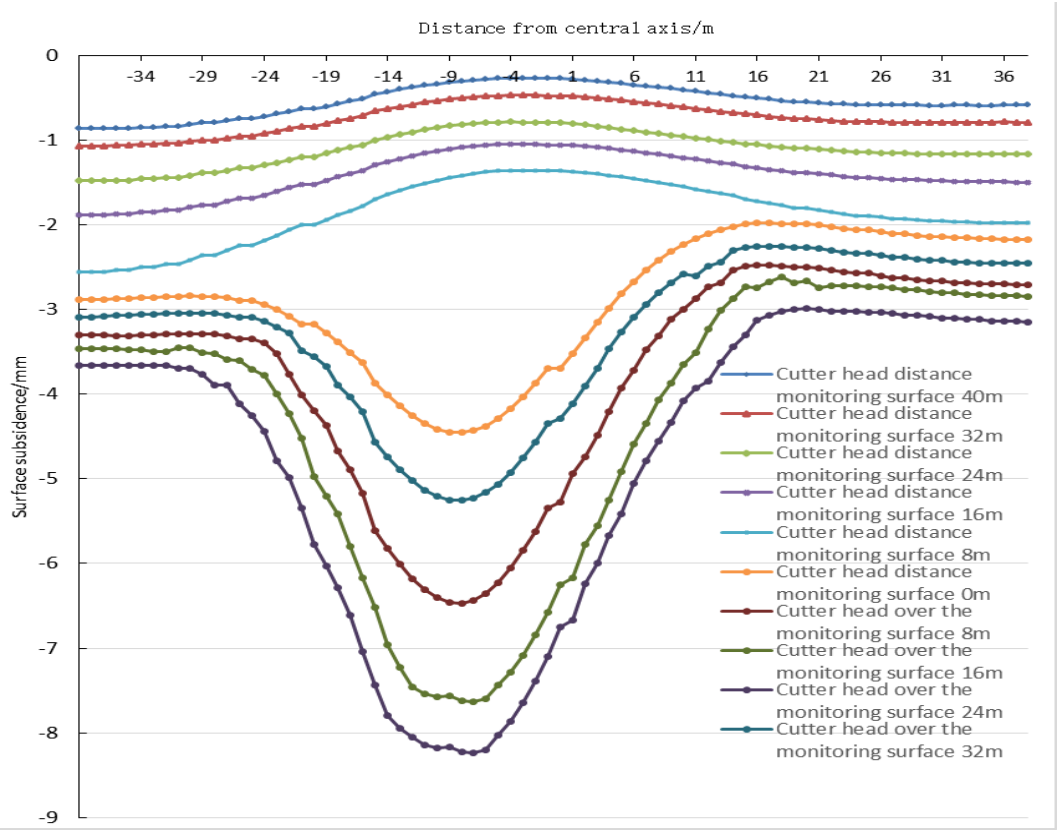

Figure 3. The horizontal monitoring surface curve of the surface excavation of the monitoring surfac

During the tunneling of the left line, a “settlement trough” symmetrical about the central axis of the tunnel will be formed on the ground. As the cutter head passes the monitoring surface farther, the depth of the settlement trough increases. The width of the settlement trough is about 32m and slightly decreases. trend. When the distance of the cutter head is about 8-40m, the settlement is smaller in the area close to the tunnel excavation compared to the far area; when the cutter head is about 0-8m away from the monitoring surface, the settlement trough It begins to form. The surface settlement of the left line vault caused by the cutterhead passing through the monitoring surface is about 36.4% of its final settlement. The surface settlement of the two tunnel axes is about 3.52mm, which accounts for about 24.28% of its final settlement. The surface settlement of the vault is about 2.42mm, which accounts for about 18.93% of its final settlement. When the cutter head passes the monitoring surface 8m, the maximum surface settlement is about 5.25mm; when the cutter head passes the monitoring surface 16m, the maximum surface settlement is about 6.45mm; when the cutter head passes the monitoring surface 34m, the maximum surface settlement is about 7.55mm; When passing the monitoring surface 32m, the maximum settlement of the ground surface is about 8.18mm. When the cutter head passed the monitoring surface for about 0-32m, the surface settlement deformation rate increased first and then gradually decreased. The width of the settlement trough increased from about 27m when it just passed the monitoring surface to about 42m.

5. Conclusion

This paper uses the PFC software numerical simulation method to analyze the stress field, displacement field, surface settlement displacement field, force analysis and conclusions of the tunnel surrounding rock under actual working conditions.

(1) The influence of shield excavation on the stress field of the surrounding rock of the tunnel. When the tunnel is excavated sequentially from left to right, the stress field around the tunnel about 2.5 times the diameter of the tunnel has a stress redistribution due to the disturbance. As the length of the

ISSN: 2414-1895 DOI: 10.6919/ICJE.202110_7(10).0080

shield tunnel increases, the degree of change in the stress field will also increase. The maximum vertical effective stress appears at the arch toe on both sides of the tunnel, and its value is about 4.89 MPa; the maximum horizontal effective stress appears at the location of the arch waist on both sides of the tunnel, and its value is about 4.43 MPa.

(2) The influence of shield excavation on the displacement field of the surrounding rock of the tunnel. During the tunneling of the shield tunnel from left to right, settlement occurred on the tunnel vault. At the front end of the shield cutterhead, due to the extrusion of the cutterhead, the ground surface will be slightly uplifted and deformed; when the cutterhead is about 16m away from the monitoring surface, a small amount of settlement begins to occur on the ground; when the cutterhead passes within about 48m of the monitoring surface, the ground surface Obvious settlement, accounting for more than 80% of the total settlement; when the cutter head passes 48m from the monitoring surface, the surface settlement basically stabilizes.

(3) The influence of shield excavation on the deformation of surrounding rock formation. Stratum deformation is mainly divided into vertical and horizontal directions. In the vertical direction, with the distance from the tunnel axis from far to nearer, the stratum deformation curve changes from the "single-peak" curve in the left-line excavation to the basically symmetrical "double-peak" curve in the right-line excavation. The surface settlement trough also gradually moved from the left to the middle of the two tunnels along with the excavation of the left and right lines; when the excavation started, the settlement was 4.16mm, and the final maximum settlement deformation was about 14.37mm. In the horizontal direction, the formation deformation mainly occurred. Near the arch waist of the tunnel, and the two sides of the two tunnels are farther apart, the deformation is slightly larger than the two sides of the closer distance. With the center of the two tunnels as the center of symmetry, it is basically "centrosymmetrical", and the maximum outer deformation is about 4.43 mm, the maximum deformation inside is about 3.34mm.

References

[1] Ren Jianxi. Research on the Deformation Law of Deep Foundation Pit Supporting Structure of Metro Station [J] Journal of Railway Engineering Society, 2009, 126(3): 89-92.

[2] Wang Mengshu. The 21st century is the era of great development of tunnels and underground space[J]. Geotechnical Engineering World, 2000(06): 13-15.

[3] Geng Xiaojie. Evaluation method and application of tunnel stability under deep buried conditions [D]. University of Science and Technology Beijing, 2015.

[4] Liu Haifeng. Numerical simulation study on mechanical properties of tunnel surrounding rock based on particle flow method[J]. Resources Information and Engineering, 2021, 36(01): 82-84+88.

[5] Gao Jingwang. Research on PFC Slope Model Construction[D]. Jilin University, 2014

[6] Wang Wei. Study on the stability of high slopes of loose accumulations based on discrete elements[D]. Chongqing Jiaotong University, 2016.

[7] Meng Jingjing. Discrete element analysis and application of rock slope stability [D]. Central South University, 2014.

[8] Zhang Guangjian, Yao Xiaobo, Hu Jin. Monitoring and numerical simulation of support axial force of foundation pit in subway transfer station[J]. Chinese Journal of Geotechnical Engineering, 2014, 36(S2): 455-459.

[9] Shen Zhifu, Jiang Mingjing, Zhu Fangyuan, Hu Haijun. The influence of discrete element microscopic parameters on sandy soil macroscopic parameters[J]. Northwest Seismology.

[10] Chen Luhai. Research on the theory of fluid-solid coupling and seepage law of underwater shield tunnels [D]. Taiyuan University of Technology, 2019.